Vol 16 No 5, May 2007
1009-1963/2007/16(05)/1327-07

Chinese Physics

© 2007 Chin. Phys. Soc.
and IOP Publishing Ltd

Angle-of-arrival fluctuations in moderate to strong turbulence

Ma Jing(马 晶), Gao Chong(高 宠)†, and Tan Li-Ying(谭立英)

National Key Laboratory of Tunable Laser Technology, Harbin Institute of Technology, Harbin 150001, *China*

(Received 18 June 2006; revised manuscript received 27 November 2006)

Based on the modified spectrum, the analytic expressions for the variance and normalized covariance of angle-of-arrival (AOA) fluctuations are presented, which are applicable to the weak and strong regimes. The experimental data of AOA fluctuations validate the new derived expressions in weak and strong regimes. The results show that the receiving aperture D, outer scale and cell scale larger than the scattering disc S contribute significantly to the AOA fluctuations, and contributions from the small-scale turbulence are negligible. For the case of $4S/D \ll 1$, the receiving aperture dominates low-pass filtering effects and the new displacement variances are in good agreement with the results from the old weak-fluctuation theory. For the case of $4S/D \gg 1$, the scattering disc dominates the low-pass filtering effects and the new displacement variances depart from the results from the old weak-fluctuation theory.

Keywords: atmospheric optics, optical wave propagation, angle-of-arrival fluctuations, moderate to strong turbulence

PACC: 4225D, 4268, 4210, 4230W

1. Introduction

The wave front tilt of optical wave propagation through atmospheric turbulence[1−3] gives rise to an angle-of-arrival (AOA) fluctuation, which is translated to a spot motion or an 'image dancing' at the focal plane of the receiver. The AOA fluctuation impairs performances of the atmospheric optical communication and atmospheric remote sensing.[4] The AOA fluctuation has been investigated for several decades.[5−13] But most of the investigations were devoted to the weak turbulence, and the AOA fluctuation in moderate to strong turbulence was little analysed. Bracewell[5] used a geometrical optics (GO) approach to calculate the AOA fluctuation. Lawrence and Strohbehn employed a Rytov approach to calculate the AOA fluctuation.[6] Their results are restricted to the weak fluctuations.

Recently a new theory has been developed for scintillation of optical wave propagating through any strength of atmospheric turbulence.[14,15] This theory is based on the Rytov approximation but modified with a filter function eliminating intermediate scales that do not contribute to the refractive and diffractive effects of propagation. This modification extends the validity of the Rytov approximation into the moderate to strong regimes as evidenced by the agreement between simulations and experimental data. It was found that this new theory was valid for the phase fluctuation.[16]

In this paper, we apply this new theory to the AOA fluctuation and develop simple analytic expressions for the variance and normalized covariance which are valid for the weak and strong regimes. An experiment to measure the AOA fluctuation has been carried out in Harbin，and these experimental data are compared with the results obtained from the new theory.

2. Theory of AOA fluctuations

2.1. The modulation process

This new theory is based on the assumption that the intensity of an optical wave is a modulation process with large-scale (refractive) eddies modulating small-scale (diffractive) eddies. In addition, the atmosphere is treated as a linear filter that serves as a spatial filter, which can account for the loss of spatial coherence of the propagating wave. The Rytov perturbation method can then be extended into the moderate and strong regimes by the introduction of a modified spectrum which filters out scales around the Fresnel size as turbulence increases. This spatial frequency filter concept is illustrated by the modified

†Corresponding author. E-mail: gaochong6@126.com

Kolmogorov spectrum[14]

$$\Phi_n(\kappa, z) = 0.033C_n^2(z)\kappa^{-11/3}[G_x(\kappa) + G_y(\kappa)], \quad (1)$$

where x and y represent large and small scales, respectively, and κ is the turbulence spectrum wave number. For horizontal paths in which the refractive-index structure parameter C_n^2 is constant, the large-scale and small-scale spatial frequency filter functions in Eq.(1) are given, respectively, by

$$G_x(\kappa) = \exp\Big(-\frac{\kappa^2}{\kappa_x^2}\Big),$$
$$G_y(\kappa) = \frac{\kappa^{11/3}}{(\kappa^2 + \kappa_y^2)^{11/6}}, \quad (2)$$

where spatial frequency filter functions only permit low-pass spatial frequencies $\kappa < \kappa_x$ or high-pass spatial frequencies $\kappa > \kappa_y$ at a given propagation distance L. The parameter $\kappa_y \sim 1/l_y$ is a small-scale spatial frequency cutoff. The parameter $\kappa_x \sim 1/S$ is a large-scale spatial frequency cutoff much like an inner-scale parameter, and S is the scattering disc scale (the diameter of the effective scattering region.[17]) In the strong regime, $l_y \sim \rho_0$, $S \sim L/k\rho_0$, ρ_0 is the coherence radius, and k is the optical wave number.

L_0 and l_0 are outer scale and inner scale, respectively. In the strong regime, $L_0 > S > l_y > l_0$, generally. With the inner scale and outer scale taken into consideration, the modified spectrum, Eq.(1) is redefined as

$$\Phi_n(\kappa) = 0.033C_n^2\Big[\frac{\exp(-\kappa^2/\kappa_x^2)}{(\kappa^2 + \kappa_0^2)^{11/6}} + \frac{\exp(-\kappa^2/\kappa_m^2)}{(\kappa^2 + \kappa_y^2)^{11/6}}\Big], \quad (3)$$

where the parameters κ_m and κ_0 are the spatial frequencies corresponding to inner scale and outer scale, respectively.

2.2. Variance of AOA fluctuations for a plane wave

Figure 1 gives the general configuration for the calculation of the AOA two-dimensional covariance. The transverse wind υ is perpendicular to the optical propagation, and β is the angle between the measurement direction (the x- axis direction) and transverse wind. Let $\alpha(\boldsymbol{r}, t)$ and $\alpha(\boldsymbol{r} + \boldsymbol{\rho}, t)$ be the AOA, with respect to the mean AOA, measured along the x-direction, at time t, and averaged over the receiving aperture D centred at positions $\boldsymbol{r}$ and $\boldsymbol{r} + \boldsymbol{\rho}$ along the transverse wind, respectively.

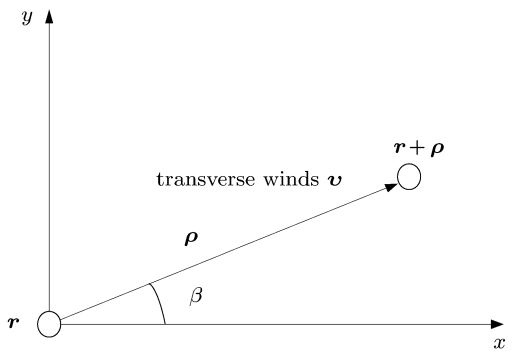


Fig.1. General configuration for the calculation of the AOA two-dimensional covariance.

The AOA covariance along the measurement direction may be obtained from the Fourier transform of the AOA spatial power spectrum for the plane wave[18,19]

$$C_\alpha(\rho, \beta) = \pi k^{-2}\int_0^\infty \kappa^3 W_\varphi(\kappa) G_{\mathrm{D}}(\kappa) \times [J_0(\rho\kappa) - \cos(2\beta)J_2(\rho\kappa)]\mathrm{d}\kappa, \quad (4)$$

where $W\varphi(\kappa)$ is the spatial power spectrum of the phase fluctuation φ; $J_p(x)$ is the Bessel function of the first kind, p denotes the order of function.

The filter function $G_D(\kappa)$ acts as a low-pass filter to remove all frequency components higher than the aperture-smoothing frequency. In order to perform the above integral, we approximate the filter function $G_D(\kappa)$ by a Gaussian pattern[20]

$$G_{\mathrm{D}}(\kappa) = \Big[2\frac{J_1(D\kappa/2)}{D\kappa/2}\Big]^2 \approx \exp[-b^2D^2\kappa^2/4], \quad (5)$$

where $b = 0.4832$ is for a best fit.

The spatial phase power spectrum for the plane wave is given by[21]

$$W_\varphi(\kappa) = 2\pi k^2\int_0^L \Phi_n(\kappa)\cos^2\Big(\frac{\kappa^2 z}{2k}\Big)\mathrm{d}z. \quad (6)$$

In terms of Eqs.(4) and (6), we can write the variance of the AOA fluctuation for the plane wave as

$$\sigma_\alpha^2 = 2\pi^2\int_0^\infty \kappa^3\Phi_n(\kappa)G_{\mathrm{D}}(\kappa)\mathrm{d}\kappa\int_0^L \cos^2\Big(\frac{\kappa^2 z}{2k}\Big)\mathrm{d}z. \quad (7)$$

By putting Eqs.(3) and (5) into Eq.(7), the AOA variance for the plane wave under the geometrical-optics approximation is obtained as

$$\sigma_\alpha^2 = 0.60C_n^2LD^{-1/3}\eta^{1/3}U[2; 7/6; 2.30\eta^2(\mu^2 + 1)] + 0.30C_n^2LD^{-1/3}\eta_{\mathrm{s}}^{1/3}U[2; 7/6; 2.30\eta_{\mathrm{s}}^2(\mu_{\mathrm{s}}^2 + 1)], \quad (8)$$

where we set the parameters $\eta_{\mathrm{s}} = D/l_y$, $\eta = D/L_0$, $\mu_{\mathrm{s}} = 2l_0/bD$ and $\mu = 2S/bD = 4.55\sqrt{L/k}(\sigma_1^2)^{3/5}D^{-1}$

as a function of Rytov variance σ_1^2. And $U(a;c;z)$ denotes the confluent hypergeometric function of the second kind.

The expression, Eq.(8), represents the strength of the AOA fluctuation arising from the large-scale and small-scale turbulences. By including the large-scale effects and neglecting the small-scale effects, Eq.(8) becomes

$$\sigma_\alpha^2 = 0.60C_n^2LD^{-1/3}\eta^{1/3}U[2;7/6;2.30\eta^2(\mu^2+1)]. \quad (9)$$

The simulation results obtained from Eqs.(8) and (9) show that the contributions of small-scale components to the AOA fluctuation for the plane wave are negligible. As the aperture increases, the difference between Eqs.(8) and (9) falls off; Their difference in all regimes is, respectively, less than 3% for the case of $D > 1$ mm and $L_0 > 1$ m, and less than 1% for the case of $D > 1$ cm. We explain these as follows: the receiving aperture filters out some of spatial high-frequency components induced by the small-scale turbulence, thereby the contributions of small-scale turbulence to the AOA fluctuation decrease with the receiving aperture increasing, and are negligible when the aperture reaches a certain value.

Since Eq.(9) is a function of the outer scale, receiving aperture and scattering disc, it determines the spatial-frequency range of the AOA fluctuation. The lower limit of the spatial frequency is determined by the outer scale that only permits high-pass spatial frequencies $\kappa > \kappa_0$; The receiver with the aperture acts as a low-pass filter to remove all frequency components higher than the spatial aperture-smoothing frequency; The spatial-frequency components induced by the cell sizes that are bounded above by the scattering disc and below by the coherence radius, do not contribute significantly to the AOA fluctuation.

For the case of $D \ll L_0$, Eq.(9) approximates

$$\sigma_\alpha^2 = 2.91C_n^2LD^{-1/3}[(1+\mu^2)^{-1/6} - 1.49\eta^{1/3}]. \quad (10)$$

For the case of $L_0 = \infty$ and $\mu \ll 1$, Eq.(9) becomes

$$\sigma_{\alpha 0}^2 = 2.91C_n^2LD^{-1/3}. \quad (11)$$

The expression, Eq.(11), agrees with the expression from the old weak-fluctuation theory in Ref.[6], when the aperture is much larger than the Fresnel zone size. We explain this as follows. The aperture smoothing dominates the low-pass filtering effects and the effect of the scattering disc is negligible for the case of $L_0 = \infty$ and $\mu \ll 1$, so Eq.(11) agrees with the expression obtained from the old weak-fluctuation theory that does not include the spatial filtering effects of atmospheric turbulence.

2.3. Variance of AOA fluctuations for a spherical wave

The spatial phase power spectrum for a spherical wave is given by[21]

$$W_\varphi(\kappa,z) = 2\pi k^2\int_0^L \Phi_n(\kappa\frac{L}{z},z)\Big(\frac{L}{z}\Big)^2 \times \cos^2\Big[\frac{\kappa^2L(L-z)}{2kz}\Big]\mathrm{d}z. \quad (12)$$

In terms of Eqs.(4) and (12), the spatial covariance of the AOA fluctuation for the spherical wave is obtained as follows:

$$C_\alpha(\rho,\beta) = 2\pi^2\int_0^L\Big(\frac{z}{L}\Big)^2\mathrm{d}z\int_0^\infty \kappa^3G_\mathrm{D}(\kappa)\Phi_n(\kappa,z) \times\cos^2\Big[\frac{\kappa^2z(L-z)}{2kL}\Big] \times[J_0(\rho\kappa)-\cos(2\beta)J_2(\rho\kappa)]\mathrm{d}\kappa. \quad (13)$$

In terms of Eqs.(3), (5) and (13), the AOA variance for the spherical wave under the geometrical-optics approximation is expressed as

$$\sigma_\alpha^2 = 0.20C_n^2LD^{-1/3}\eta^{1/3}U[2;7/6;2.30\eta^2(\mu^2+1)], \quad (14)$$

where we set

$$\mu = 2S/bD = 7.81\sqrt{L/k}\beta_0^{6/5}D^{-1}$$

as a function of $\beta_0 = (0.5C_n^2k^{7/6}L^{11/6})^{1/2}$.

Simulation results show that contributions of small-scale components to the AOA fluctuation of the spherical wave in all regimes are less than 2% for the case of $D > 1$ cm, due to the aperture-smoothing effect. So Eq.(14) including large-scale turbulence and neglecting the small-scale turbulence is valid for the spherical wave.

For the case of $D \ll L_0$, Eq.(14) approximates

$$\sigma_\alpha^2 = 0.97C_n^2LD^{-1/3}[(1+\mu^2)^{-1/6} - 1.49\eta^{1/3}]. \quad (15)$$

For the case of $L_0 = \infty$ and $\mu \ll 1$, Eq.(14) becomes

$$\sigma_{\alpha 0}^2 = 0.97C_n^2LD^{-1/3}. \quad (16)$$

In the weak regime, the AOA variance for the spherical wave under the geometrical-optics approximation is given by[6]

$$\sigma_{\alpha 0}^2 = 1.05C_n^2LD^{-1/3},$$

$$D \gg \sqrt{L/k}. \tag{17}$$

We see that the new expression, Eq.(16), approximates the expression, Eq.(17).

2.4. Spatial covariance of AOA fluctuations

In the following analysis, we develop the expression of the normalized covariance for the case of $L_0 = \infty$. The expressions of the normalized covariances for the plane wave and spherical wave, obtained by using the geometrical-optics approximation are agreeable.

By inserting Eqs.(3), (5) and (6) into Eq.(4), the analytical solution for the normalized covariance is obtained as

$$b_\alpha(\rho,\beta) = \frac{C_\alpha(\rho,\beta)}{\sigma_\alpha^2} = {}_1F_1\Big(1/6;1;-\frac{d^2}{1+\mu^2}\Big) - 0.02\cos(2\beta)\frac{d^2}{1+\mu^2}\,{}_1F_1\Big(7/6;3;-\frac{d^2}{1+\mu^2}\Big), \tag{18}$$

where we set $d = \rho/bD$. ${}_1F_1\ (a;c;z)$ denotes a confluent hypergeometric function.

From Eq.(18), we see that the normalized covariance depends on d and μ. The angle β between the measurement direction and transverse wind has an influence on the normalized covariance of the AOA fluctuation.

Figure 2 shows the longitudinal ($\beta = 0°$) and transverse ($\beta = 90°$) normalized covariances and their difference. The fastest decorrelation of the AOA fluctuation along the longitudinal direction in the strong regime is clearly seen. In Fig.3 the normalized covariance function is shown for different values of μ. We see that the longer correlation tail for a stronger turbulence is characterized by the scattering disc.

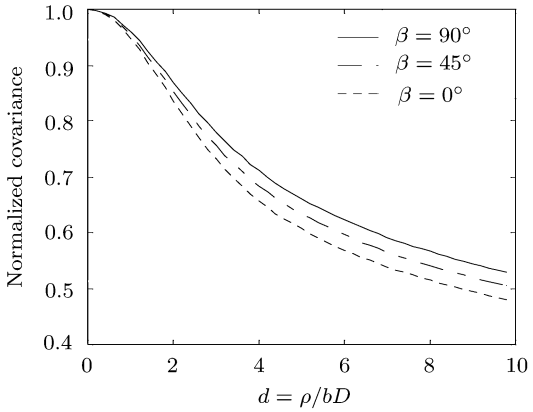


Fig.2. Normalized covariance vs ρ/bD for different angles of β and $\mu = 2$.

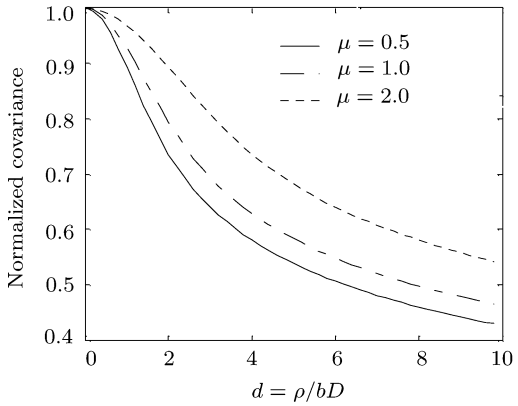


Fig.3. Normalized covariance vs ρ/bD for different values of μ and $\beta = 45°$.

3. Analysis of simulation

Now we analyse the range of validity for the displacement variances. In the following analysis we take the wavelength $\lambda = 0.532$ μm, propagation distance $L = 30$m–4.3 km, and refractive-index structure parameter $C_n^2 = 10^{-13}$ m$^{-2/3}$.

In Figs.4 and 5 we compare the displacement variances assumed to be valid in all the regimes for the plane wave and spherical wave, Eqs.(9) and (14), respectively, with the weak-fluctuation-theory results, Eqs.(11) and (17), that are valid in the weak regime. Curves plotted in Figs.4 and 5 are obtained in the case of $L_0 = \infty$.

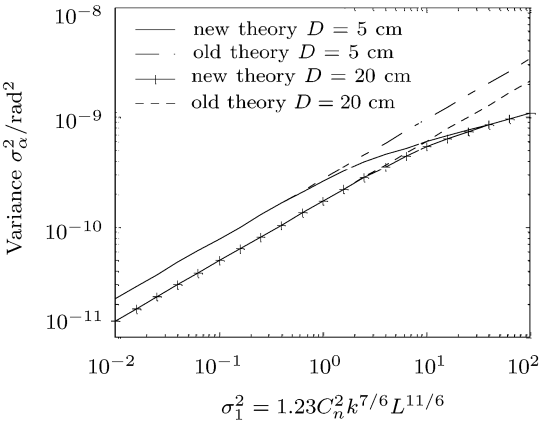


Fig.4. Variance of AOA fluctuation for the plane wave vs Rytov variance σ_1^2 for different apertures.

Figures 4 and 5 show that for the case of $D = 5$ cm these displacement variances agree with the previous weak-fluctuation-theory results in the weak fluctuation regime, $\sigma_1^2 < 1$ or $\beta_0^2 < 1$, and that they are

separated as the fluctuations move into the moderate ($\sigma_1^2 \sim 1$ or $\beta_0^2 \sim 1$) and strong ($\sigma_1^2 > 1$ or $\beta_0^2 > 1$) regimes. For the case of $D = 20$ cm these displacement variances agree with previous results in the moderate regime, but they are separated in a stronger turbulence. When $\sigma_1^2 > 10$ or $\beta_0^2 > 10$, the aperture-smoothing effect may be negligible and the results obtained by new displacement variances for the apertures of 5 cm and 20 cm are agreeable.

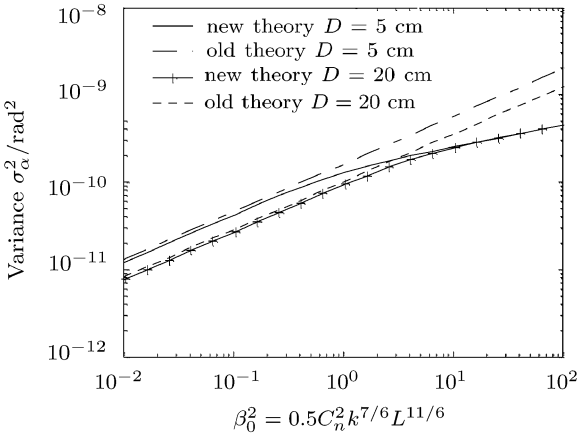


Fig.5. Variance of AOA fluctuation for the spherical wave vs β_0^2 for different apertures.

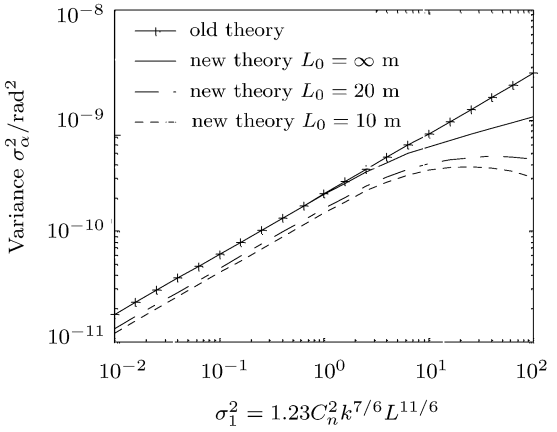


Fig.6. Variance of AOA fluctuation for the plane wave vs σ_1^2 for different outer scales and the aperture of $D = 10$ cm.

Figures 6 and 7 show the effect of outer scale on the AOA fluctuation. We see that as the turbulence strength increases, the displacement variances, Eqs.(9) and (14) including the outer scale, predict lower values for the AOA fluctuation of the plane wave and spherical wave than the weak-fluctuation-theory results, Eqs.(11) and (16); and that as the separation increases, with the outer scale included, there occurs a similar effect.

In Figs.8 and 9, we analyse the effects of the values of $\eta = D/L_0$ and $\mu = 2S/bD$ on displacement variances, Eqs.(9) and (14), respectively, normalized by the weak-fluctuation-theory results, Eqs.(11) and (16). The displacement variances normalized by the weak-fluctuation-theory results are agreeable for the plane wave and spherical wave.

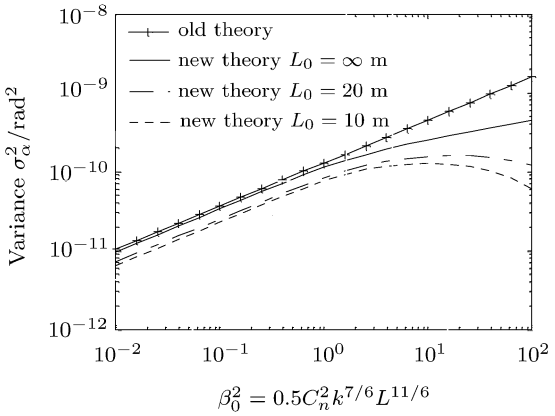


Fig.7. Variance of AOA fluctuation for the spherical wave vs β_0^2 for different outer scales and the aperture $D = 10$ cm.

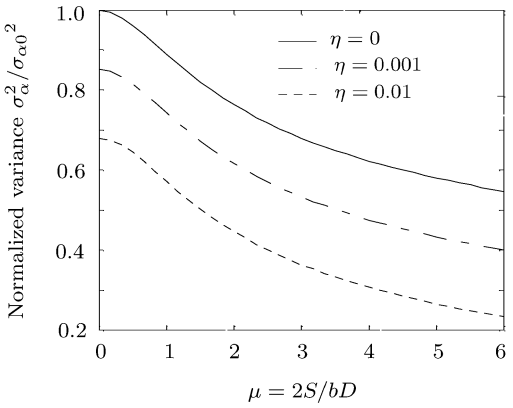


Fig.8. Ratio of the displacement variance σ_α^2 to weak-fluctuation result $\sigma_{\alpha 0}^2$ as a function of the ratio μ for different values of η.

Figure 8 shows the normalized displacement variance plotted as a function of μ for different values of η. The curves indicate that for the case of $\mu \gg 1$ the weak-fluctuation-theory variance significantly overestimates the displacement variance and the saturation effect of the AOA fluctuation occurs, but for the case of $\mu \ll 1$ the weak-fluctuation-theory result is a good approximation. Figure 9 shows the normalized displacement variance plotted as a function of η for different values of μ. The curves indicate that the

normalized displacement variance decreases with the value of η increasing.

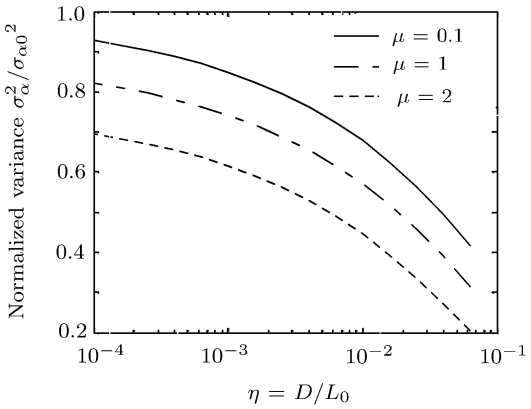


Fig.9. Ratio of the displacement variance σ_α^2 to weak-fluctuation result $\sigma_{\alpha 0}^2$ as a function of the ratio η for different values of μ.

4. Experimental analysis

A measurement of the AOA fluctuation in a free-space laser transmission experiment has been carried out over a three-month period in Harbin. The transmitter of the experiment is a highly coherent single-mode 10 mW laser emitting CW at a 532 nm wavelength. A radially symmetrical beam is transmitted with the stability of $\pm 1\%$ and beam waist radius of 1 mm. The receiver shown in Fig.10 is composed of the optical telescope, optical filter, total reflection mirror, attenuator, CMOS lens and CMOS sensor (BASLER A602f), which are mounted on a three-dimensional adjusting optical platform. The BASLER A602f model of scan CMOS camera has an important feature of very high frame rate and sensitivity. A pixel size of the CMOS sensor is 9.9 μm(H) $\times$9.9 μm(V). The fast region of interest, centroid window of 10 $\times$10 pixels, is used to achieve a high sampling rate of 1 kHz. The aperture and magnification factor of the receiving optical telescope are 60 mm and 19, respectively. The aperture and focal length of the CMOS lens are 28 mm and 50 mm, respectively.

The light propagating 3200 m in path on the average 35 m above the ground is received by the optical telescope, and impinges upon the focal-plane CMOS sensor with an effective focal length of 950 mm. At the receiver, beam diameter is 2.6 m, which is much larger than the receiving aperture. The receiving aperture is two times smaller than atmospheric coherence length.

The beam arriving at the aperture of the receiver exhibits the AOA fluctuations that are translated to a spot motion or an 'image dancing' at the focal plane. The experimental data of AOA fluctuations are obtained by measuring the random shifts at central location of the image on the focal-plane CMOS sensor. Above all, we analyse the spot profile at the focal plane. Figure 11 shows the profile of the typical focal spot in centroid window of 10×10 pixels.

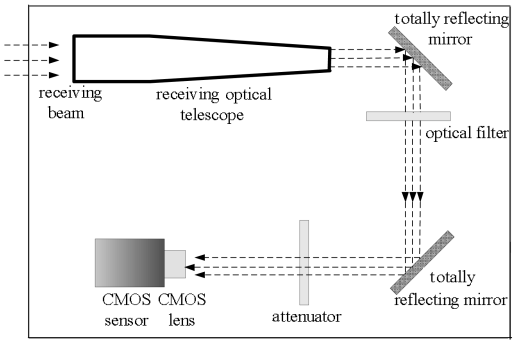


Fig.10. Simplified block diagram of the experimental receiver.

Figure 11 shows that the spot on the focal-plane CMOS sensor is not subjected to severe atmospheric degradation and the spot profile approximates a Gaussian profile. We give the above results an expression that the aperture is two times smaller than atmospheric coherence length, causing mostly shifts at the spot location.

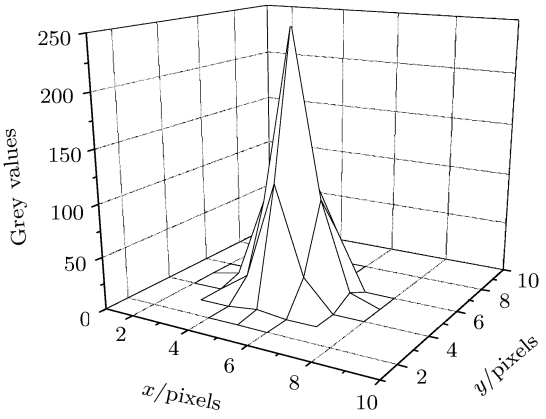


Fig.11. Spot profile on the focal-plane CMOS sensor.

Now we compare the results, Eqs.(10) and (11), with the experimental data. The curves a and b in Fig.12 are obtained from Eqs.(10) and (11), respectively. Dots in Fig.12 represent the experimental data.

We see in Fig.12 that the experimental data are in good agreement with Eq.(10) derived by the new theory, including the outer scale $L_0 = 15$ m, but depart from Eq.(11) given by the old theory when the standard deviation of the AOA fluctuation is over 15 μrad.

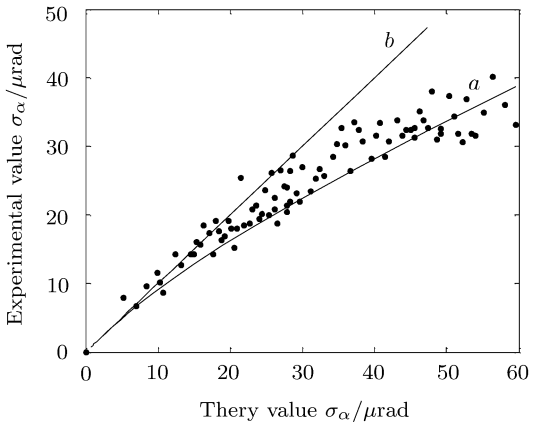


Fig.12. Comparison of the theoretical results with the experimental data. Curve a from Eq.(10), curve b from Eq.(11).

5. Conclusions

The modified Rytov theory introduced by Andrews *et al* has been developed for scintillation. In this paper we have applied this modified Rytov theory to the AOA fluctuation and developed simple analytic expressions for the displacement variances of the AOA fluctuation associated with horizontal paths, which are applicable to weak and strong regimes. In addition to the variance of the AOA fluctuation, this method also leads to expressions for the covariance function.

The receiving aperture has smoothing effects and filters out spatial high-frequency components induced by the small-scale turbulence. Simulation results show that effects of small-scale turbulence and inner scale on the AOA fluctuation in all regimes are negligible. When the receiving aperture $D > 1$ cm, their contributions to the AOA fluctuation in all regimes are less than 1% and 2%, respectively, for the plane wave and spherical wave. Contributions of the aperture, outer scale and cell scale larger than the scattering disc to the AOA fluctuation are significant.

It is evidenced that the new displacement variances extending into the weak regime are also valid. These displacement variances agree with the previous weak-fluctuation-theory results in the weak fluctuation regime. When the aperture $D < 20$ cm and turbulence strength in a very strong regime, $\sigma_1^2 > 10$ or $\beta_0^2 > 10$, the aperture-smoothing effect is negligible and the results obtained by new displacement variances for the different apertures are agreeable.

For the case of $4S/D \gg 1$, the scattering disc dominates the low-pass filtering effects, the old weak-fluctuation-theory results overestimate the new displacement expressions, and the saturation effect occurs. For the case of $4S/D \ll 1$, the aperture-smoothing effect dominates the low-pass filtering effects, the new displacement expressions are in good agreement with the weak-fluctuation-theory results, and the saturation effect does not occur.

Furthermore, a measurement of the AOA fluctuation has been carried out, and these experimental data are in good agreement with the results obtained by the new theory in all regimes.

References

[1] Chen J Y, Chen S G and Wang G R 2005 *Acta Phys. Sin.* **54** 3123 (in Chinese)
[2] Ji X L, Huang T X and Lu B D 2006 *Acta Phys. Sin.* **55** 978 (in Chinese)
[3] Dai X G, Fu C B and Wang P 2005 *Chin. Phys.* **14** 850
[4] Liao T H and Gao Q 2006 *Chin. Phys.* **15** 347
[5] Churnside J H 1965 *J. Opt. Soc. Am.* A **6** 275
[6] Lawrence R S and Strohbehn J W 1970 *Proc. IEEE* **58** 1523
[7] Song Z F, Ma J and Liu X C 1992 *Proc. SPIE* **1628** 239
[8] Fante R L 1975 *Proc. IEEE* **63** 1669
[9] Mironov V L, Pokasov V V and Chen B N 1980 *Radiophys. Quantum. Electron.* **23** 319
[10] Belenkii M S and Shelekhoy A P 1984 *Radiophys. Quantum. Electron.* **26** 1096
[11] Andrews L C and Phillips R L 1998 *Laser Beam Propagation through Random Media* (Bellingham Washington: SPIE Optical Engineering Press) p223
[12] Borgnino J, Martin F and Ziad A 1992 *Opt. Commun.* **91** 267
[13] Couto D M and Cole R S 1996 *Electron. Lett.* **32** 237
[14] Andrews L C, Phillips R L, Hopen C Y and Al-Habash M A 1999 *J. Opt. Soc. Am.* A **16** 1417
[15] Andrews L C, Phillips R L and Hopen C Y 2000 *Opt. Eng.* **39** 3272
[16] Young C Y, Masino A J and Thomas F 2003 *Proc. SPIE* **4976** 141
[17] Frehlich R G 1987 *J. Opt. Soc. Am.* A **4** 360
[18] Roddier F 1981 *The Effect of Atmospheric Turbulence in Optical Astronomy* (Amsterdam: North-Holland Press) p281
[19] Conan R, Borgnino J and Ziad A 2000 *J. Opt. Soc. Am.* A **17** 1807
[20] Haddon J and Vilar E 1986 *IEEE Trans. Antennas Propagation* **34** 646
[21] Wolfe W L and Zissis G J 1978 *The Infrared Handbook* (Washington: Office of Naval Research) p61